Geoscientific Model Development Discussions

The regional aerosol-climate model REMO-HAM

J.-P. Pietikäinen[1,2,3], D. O'Donnell[1], C. Teichmann[2,3], U. Karstens[4], S. Pfeifer[3], J. Kazil[5], R. Podzun[2,3,†], S. Fiedler[6], H. Kokkola[1], W. Birmili[7], C. O'Dowd[8], U. Baltensperger[9], E. Weingartner[9], R. Gehrig[10], G. Spindler[7], M. Kulmala[11], J. Feichter[2], D. Jacob[2,3], and A. Laaksonen[1,12]

[1]Finnish Meteorological Institute, P.O. Box 503, 00101 Helsinki, Finland
[2]Max Planck Institute for Meteorology, Bundesstrasse 53, 20146 Hamburg, Germany
[3]Climate Service Center, Chilehaus – Eingang B, Fischertwiete 1, 20095 Hamburg, Germany
[4]Max Planck Institute for Biogeochemistry, Hans-Knöll-Straße 10, 07745 Jena, Germany
[5]Cooperative Institute for Research in Environmental Sciences (CIRES), University of Colorado, 325 Broadway R/CSD Boulder, Colorado, USA
[6]Institute for Climate and Atmospheric Science, University of Leeds, LS2 9JT, Leeds, UK
[7]Leibniz Institute for Tropospheric Research (IfT), Permoserstr. 15, 04318 Leipzig, Germany
[8]National University of Ireland Galway, University Road, Galway, Ireland
[9]Laboratory of Atmospheric Chemistry, Paul Scherrer Institute, 5232 Villigen PSI, Switzerland
[10]Empa – Swiss Federal Laboratories for Materials Science and Technology, Überlandstrasse 129, 8600 Dübendorf, Switzerland
[11]Department of Physics, University of Helsinki, P.O. Box 44, 00014, Helsinki, Finland

[12]Department of Applied Physics, University of Eastern Finland, P.O. Box 1627, 70211 Kuopio, Finland
[†]Deceased in September 2011

Correspondence to: J.-P. Pietikäinen (joni-pekka.pietikainen@fmi.fi)

Title Page

Abstract | Introduction

Conclusions | References

Tables | Figures

|◄ | ►|

◄ | ►

Back | Close

Full Screen / Esc

Printer-friendly Version

Interactive Discussion

Abstract

REMO-HAM is a new regional aerosol-climate model. It is based on the REMO regional climate model and includes all of the major aerosol processes. The structure for aerosol is similar to the global aerosol-climate model ECHAM5-HAM, for example the aerosol module HAM-M7 has been coupled with a two-moment stratiform cloud scheme. In this work, we have evaluated the model and compared the results against ECHAM5-HAM and measurements. Four different measurement sites was chosen for the comparison of total number concentrations, size distributions and gas phase sulfur dioxide concentrations: Hyytiälä in Finland, Melpitz in Germany, Mace Head in Ireland and Jungfraujoch in Switzerland. REMO-HAM is run with two different resolutions: $50 \times 50 \, \text{km}^2$ and $10 \times 10 \, \text{km}^2$. Based on our simulations, REMO-HAM can represent the measured values reasonably well. The total number concentrations are slightly underestimated, which is probably due to the missing boundary layer nucleation and online secondary organic aerosol model. The differences in the total number concentrations between REMO-HAM and ECHAM5-HAM can be mainly explained by the difference in the nucleation mode. From the meteorological point of view, REMO-HAM represents the precipitation fields and 2 m temperature profile very well compared to measurement. Overall, we have shown that REMO-HAM is a functional aerosol-climate model, which will be used in further studies.

1 Introduction

Aerosol particles have an important role in the climate system. They have the ability to scatter and absorb both solar and thermal radiation. These processes are referred to as the direct effect of aerosols (Haywood and Boucher, 2000). Absorbing aerosol particles can also heat the surrounding air, which can lead to evaporation of cloud droplets. This is an effect referred as semi-indirect effect (Hansen et al., 1997). Finally, the ability to act as cloud condensation nuclei (CCN) and ice nuclei (IN) is referred as

the indirect effect of aerosol particles (Lohmann and Feichter, 2005). Indirect effect is usually divided into two parts: cloud albedo effect (increment in aerosol concentrations leads to increment in cloud droplets, which increases the albedo) and cloud lifetime effect (increment in aerosol concentrations leads to smaller droplets, which reduced precipitation efficiency and prolongs the cloud lifetime). The aerosol effects have been widely studied experimentally and with models. However, the uncertainty of aerosols related to aerosol-cloud interactions still remains quite high (IPCC, 2007).

Aerosol particles originate both from natural and anthropogenic sources (Seinfeld and Pandis, 1998). Tropospheric aerosol particles are either formed from the gas phase through nucleation and growth, or directly emitted from the surface of Earth. Downward mixing of aerosol particles from the stratosphere has a minor contribution to tropospheric aerosol loads. Kulmala et al. (2004) showed that nucleation events occur frequently around the globe and that the nucleation has a significant role in the (regional) CCN concentrations. For the emitted particles, major sources are oceans, arid and semi-arid regions, volcanoes, wildfires and combustion of fossil and biomass fuels (Dentener et al., 2006).

Many of the aerosol processes have strong regional characteristics. Sogacheva et al. (2005, 2007) showed that nucleation events occur more frequently in Hyytiälä, Finland, if the incoming air masses come from the Arctic Ocean rather than from Central Europe. This is interesting, because the nucleation is a frequent process in Central Europe, and we don't know what suppresses nucleation when air flows towards Scandinavia. The atmospheric dynamics influence the properties of aerosol particles, but on the other hand, the local aerosol processes change the number concentrations and size distributions, which leads to changes of the dynamics. Laaksonen et al. (2005) showed that at Po Valley, Italy, nucleation may contribute up to a third to the regional CCN budget. Moreover, Raatikainen et al. (2010) reported that aerosol particle volume increases with the increment of population along the parcel trajectory. This shows the importance of emissions to the atmospheric aerosol properties.

The aerosol effects on warm clouds have been considered in climate models for years (Jones et al., 1994). The first climate models used sulfate aerosols as a surrogate for all anthropogenic aerosols. During the development of the climate models, the major global aerosol components (such as sulfate, particulate organic matter, black carbon, sea salt and mineral dust) have been included (Stier et al., 2005). Different approaches to describe the aerosol distribution have been implemented, for example a modal presentation by Stier et al. (2005) and a sectional presentation by Kokkola et al. (2008). Aerosol modules are used in global (Stier et al., 2005) and regional (Zubler et al., 2010) climate models with a coupling to the models' cloud scheme (Lohmann et al., 2007).

Recently, many modeling efforts have been made to study the aerosol-cloud-interactions on different scales (Langmann et al., 2008; Lohmann et al., 2007; Spracklen et al., 2006; Stier et al., 2005; Makkonen et al., 2009; Zubler et al., 2010; O'Donnell et al., 2011). In this work, we present the new regional aerosol-climate model REMO-HAM, which is suitable for studying aerosol-cloud-interactions on a regional scale. It is based on the REMO regional climate model by Jacob and Podzun (1996). In this paper, we will concentrate to evaluate the REMO-HAM model against measurements, and compare it against the global aerosol-climate model ECHAM5-HAM.

2 Model description

2.1 General circulation model ECHAM5-HAM

The global climate model ECHAM5-HAM (Roeckner et al., 2003; Stier et al., 2005) has been used in this study to provide lateral aerosol boundary data for the regional model simulations, and to provide data for model comparison. ECHAM5-HAM includes the aerosol microphysics module HAM (Stier et al., 2005) as well as the microphysical module M7 (Vignati et al., 2004). The aerosol model has been coupled with a double-moment cloud scheme (e.g., Lohmann et al., 2007). During the following sections, more detailed information about the different modules will be provided.

The regional aerosol-climate model REMO-HAM

J.-P. Pietikäinen et al.

Full Screen / Esc

Printer-friendly Version

Interactive Discussion

2.2 The REMO model

The regional model REMO is a hydrostatic, three-dimensional atmosphere model, that has been developed at the Max-Planck-Institute for Meteorology in Hamburg. It is based on the Europa Model, the former numerical weather prediction model of the German Weather Service (for more details, see Jacob and Podzun, 1996; Jacob, 2001). The physical core of REMO is based on the physical package of the global circulation model ECHAM4 (Roeckner et al., 1996). Prognostic variables are the horizontal wind components, surface pressure, temperature, specific humidity, cloud liquid water and ice. The vertical levels in REMO are represented in a hybrid coordinate system. Hybrid coordinates follow the surface orography in the lower levels and become independent from surface orography at higher atmospheric model levels.

In REMO, the stratiform (large-scale) cloud scheme is based on the original ECHAM4 cloud scheme (details from Roeckner et al., 1996) and has been updated following ECHAM5 by Pfeifer (2003). The scheme includes prognostic equations for cloud water, water vapor and cloud ice, and has an empirical cloud cover scheme by Sundqvist et al. (1989). The cloud droplet number concentration is parameterized separately for continental and maritime climate, and it is a function of height (Roeckner et al., 1996).

The convective (sub-grid) cloud parameterization is based on mass-flux scheme from Tiedke (1989) with modifications by Nordeng (1994). Pfeifer (2003) also included a new type of convection to the cloud scheme, the so called cold convection. This type of convection might occur in cold air outbreaks over sea in the extra tropical atmosphere.

REMO does not include an aerosol module. The information about aerosols, for example in the radiation scheme, is based on the climatology from Tanre et al. (1984). In this climatology, the spatial distributions of the optical thickness of land, sea, urban, and desert aerosols, and well mixed tropospheric and stratospheric background aerosols are presented. The climatology is based on a global T10 spectral distribution

(1300 km, fixed in time) and the aerosols in this climatology have no direct influence on the clouds, that is, the indirect aerosol effects are not represented.

2.3 Aerosol physics and chemistry

HAM-M7 is an aerosol chemistry and physics model, which predicts the evolution of an ensemble of microphysically interacting internally- and externally-mixed aerosol population as well as their size-distribution and composition. The size-distribution is represented by a superpositioning of seven log-normal modes. The M7 microphysical core includes the following processes: coagulation, condensation, nucleation, thermodynamic equilibrium with water vapor and the inter modal transfer. A detailed description of the HAM-M7 model can be found in Stier et al. (2005) and Vignati et al. (2004). In the following, we will present the main features of the aerosol model.

The seven log-normal modes are: soluble and insoluble Aitken, accumulation and coarse mode, and one soluble nucleation mode. Table 1 shows how HAM-M7 treats different species. The five aerosol components considered in HAM-M7 are sulphate, black carbon, organic carbon, sea salt and mineral dust. These component have been divided into different modes as shown in Table 1. The aerosol dynamics, e.g. coagulation, can change the composition of each internally mixed mode. The HAM-M7 has two water uptake methods: calculating the equilibrium liquid water content of the aerosol using the ZSR method Jacobson et al. (1996), and the second one is based on Kappa-Köhler theory (Petters and Kreidenweis, 2007; O'Donnell et al., 2011).

In the framework of this work, four different nucleation schemes have been included. The binary sulfuric acid – water based nucleation methods are by Vehkamäki et al. (2002) and Kazil and Lovejoy (2007). Furthermore, two nucleation methods have been implemented for the forested boundary layer: nucleation based on cluster activation following Kulmala et al. (2006) and nucleation based on kinetic activation following Laakso et al. (2004). Newly formed particles (number and mass) are committed to the nucleation mode. Nucleation has been restricted to happen only in the cloud-free

portions of the model grid volumes. In cloudy portions, sulfuric acid is removed by condensation.

In our current setup, we use a sulfate aerosol chemistry module described by Feichter et al. (1996). In this approach, dimethyl sulfide (DMS), sulfur dioxide (SO_2) and sulfate (SO_4^{2-}) are treated as prognostic variables. We use the three dimensional monthly mean oxidant fields for hydroxyl (OH), hydrogen peroxide (H_2O_2), ozone (O_3) and nitrogen dioxide (NO_2) (Stier et al., 2005). These fields originate from the calculations of comprehensive MOZART chemical transport model (Horowitz et al., 2003). The chemical module calculates the oxidation in the gas- and aqueous phase. In the gas phase, SO_2 and DMS are oxidized by OH and DMS reacts with the nitrate radical (NO_3). The oxidation of O_3, SO_2 and H_2O_2 are considered in the aqueous phase. The gas phase sulfuric acid concentration is calculated with an improved time integration scheme by Kokkola et al. (2009).

2.3.1 Emissions used in the model

The emission module is based on the AEROCOM emission inventory for the year 2000 excluding the sea salt emissions and Dimethyl Sulphide (DMS) emissions (Dentener et al., 2006). The sea salt (SS) emissions are based on the approach by Stier et al. (2005). In this approach, the emissions of sea salt particles are based on a look-up table for wind speeds between 1 and $40\,m\,s^{-1}$. All the emission species, except the sulfur compounds, are treated as primary emissions. In addition, the DMS emissions from marine biosphere are calculated based on DMS sea water concentrations using the air-sea exchange rate. This has been calculated using the model's 10 m wind speed information. The terrestrial biogenic emissions (DMS) are prescribed (for details of both DMS emission methods, please see Stier et al., 2005).

The AEROCOM emissions are presented on a 1.0° global grid. For all of the compounds, the data is preprocessed using a 1st order conservative remapping method. The data is remapped to the grid used in REMO and read in once per modeled month. We assume homogeneous mixing across the model grid box for all aerosol

The regional aerosol-climate model REMO-HAM

J.-P. Pietikäinen et al.

species. The emissions are injected to the lowest model layer, except for biomass burning emissions, explosive and continuous volcanoes, and emissions coming from industry, shipping and power plants. For all of the vertically dependent emissions, the levels described by Dentener et al. (2006) are being used. For detailed infor-
5 mation of different AEROCOM species, please see Dentener et al. (2006) or visit http://nansen.ipsl.jussieu.fr/AEROCOM/.

In the following, we describe the aerosol emission in the model. Details on the sources can be found in Dentener et al. (2006). Sulfur (S) has been divided between gas phase (97.5 %) and particles (2.5 %) as primary SO_4 (sulfate). For industry, ship-
10 ping and power plants emissions, 50 % of the sulfate emissions are released to the accumulation mode and 50 % to the coarse mode. The remaining sulfate emissions are divided between Aitken mode (50 %) and accumulation mode (50 %). Secondary Organic Aerosol (SOA) formation is based on biogenic monoterpene emissions assuming a fixed SOA yield (15 %), and that the formation is taking place in the emitting
15 gridbox. The Primary Organic Matter (POM) emissions has been released to organic carbon. The mass ratio of organic mass to organic carbon is 1.4. 65 % of SOA and POM emissions are assumed to be soluble and 35 % insoluble. The insoluble organic matter is released entirely to Aitken mode. Soluble orgnanic matter is emitted to organic carbon, except fire and fuel emissions, is divided between Aitken and accumulation mode
20 (50 % to each). The fire POM emissions are released to the soluble accumulation mode and fuel emissions to the soluble Aitken mode. All black carbon emissions are released to the insoluble Aitken mode. For dust emissions, we use prescribed AEROCOM mass fluxes. These fluxes are on a monthly scale and have separate fields for accumulation and coarse mode (the mode paramameters are the same as in M7).

25 ## 2.4 Cloud microphysics

The stratiform cloud scheme described in Sect. 2.2 calculates the number of cloud droplets separately for maritime and continental clouds. The calculation does not take into account the information about aerosols provided by the HAM aerosol module. One

Title Page

Abstract | Introduction

Conclusions | References

Tables | Figures

◄ | ►►

◄ | ►

Back | Close

Full Screen / Esc

Printer-friendly Version

Interactive Discussion

way to use the aerosol information is to use the approach by Lohmann and Roeckner (1996), where the cloud droplet concentration for continental and marine clouds is calculated from the aerosol sulfate mass. This approach corrects the values calculated by the normal scheme but still does not fully take account of the information provided by the aerosol module. In order to use the information in the stratiform clouds, a new double-moment cloud microphysics scheme was implemented (Lohmann and Roeckner, 1996; Lohmann and Kärcher, 2002; Lohmann et al., 2007). The new scheme has prognostic equations for water vapor, cloud water and cloud ice. In addition, it has prognostic equations for cloud droplet number concentration (CDNC) and ice crystal number concentration (ICNC). It uses bulk cloud microphysics (Lohmann and Roeckner, 1996), and a fractional cloud cover by Sundqvist et al. (1989). In the approach by Sundqvist et al. (1989), the relative humidity determines whether cloud is formed in the grid box or not. The autoconversion of cloud droplets can be calculated with two different parameterizations: Beheng (1994) and Khairoutdinov and Kogan (2000). The cloud scheme also includes a cirrus parameterization from Lohmann and Kärcher (2002).

The new cloud scheme has been fully coupled with the HAM-M7 aerosol module. To connect the information from the aerosol module to the CCN activation, the activation schemes from Lin and Leaitch (1997) and Abdul-Razzak and Ghan (2000) have been implemented. In this study, the latter has been used. To connect the calculated cloud droplet and ice crystal number concentrations to the radiation, the approach by Lohmann et al. (2007) for cloud droplets and the approach by Lohmann et al. (2008) for ice crystals have been implemented. In these approaches, using the CDNC and ICNC information combined with the cloud liquid water/ice content, the effective radius of droplets/crystal is calculated and passed to the radiation.

2.5 Tracer transport

The tracers of the model undergo the following transport processes: transport in convective clouds, sedimentation, dry- and wet deposition, vertical diffusion and vertical- and horizontal advection. The convective transport of tracers is based on the mass-

flux scheme described in Sect. 2.2. The sedimentation velocity calculation is based on the Stokes velocity with the Cunningham slip-flow correction factor accounting for non-continuum effects (Stier et al., 2005). The dry deposition is based on the same size-dependent parameterization as in the ECHAM5-HAM model (Stier et al., 2005).

5 For the wet deposition, we have implemented two different approaches for below-cloud aerosol scavenging. The first one, by Stier et al. (2005), can be used, but also the size dependent below-cloud scavenging by rain, or by rain and snow, by Croft et al. (2009) has been introduced and used in this work. The vertical diffusion fluxes due to sub grid scale turbulence are calculated for the lowest layer (surface layer) according to Louis

10 (1979). For the other layers, a second-order closure scheme of hierarchy level 2 by Mellor and Yamada (1974), is used. For the horizontal and vertical advection, we have implemented the finite difference, antidiffusive scheme proposed by Smolarkiewicz (1984, 1983). The scheme is mass conserving, positive definite and computationally efficient. The monotonicity is achieved by using higher order flux corrections. We also use two

15 corrective steps (using antidiffusion velocity) in order to decrease the numerical diffusion (for details, see Langmann, 2000; Smolarkiewicz, 1983, 1984).

2.5.1 Lateral and upper boundary

For the meteorological part, the model uses at the lateral boundary the relaxation scheme by Davies (1976). In this scheme, the eight outermost grid boxes are adjusted

20 with an exponentially decreasing function. The influence of the large-scale driving fields decreases when moving towards the domain center. For the aerosol part, the lateral boundary treatment of tracers is implemented after Pleim et al. (1991). Due to discontinuities of the advection flux fields and the concentration fields at the boundaries, the lateral boundaries would have upstream reflections near the outflow boundary. The

25 approach by Pleim et al. (1991) minimizes these discontinuities by setting the the flux divergence to zero in the grid boxes next to the boundary.

We have used the European Centre for Medium-Range Weather Forecasts (ECMWF) operational data set for the meteorological data at the model domain bound-

aries. The aerosol data is from ECHAM5-HAM which has been run for the needed time period nudging (assimilation by linear relaxation) the model towards the ECMWF data. The ECHAM5-HAM global output has been conservatively remapped to the REMO grid using Climate Data Operators (CDO) program (https://code.zmaw.de/projects/cdo/).

5   We have also done the remapping for the vertical levels due to the better presentation of orography.

2.5.2   Dynamical downscaling

The resolution of ECHAM5-HAM used in this study was T63L31 with a time step of 720 s. This resolution corresponds to the resolution of 1.9° (horizontally ~210 km).

10   A jump from 1.9° resolution to the resolution used in this study, 0.088° ($10 \times 10 \, km^2$) is too large. In order to overcome this problem, dynamical downscaling method was used (also known as the double-nesting method). In this method, the model is run with an intermediate resolution and the results from this simulation are used as a boundary data for the higher resolution simulation. We have used the resolution of 0.44° ($50 \times 50 \, km^2$)

15   for the intermediate step.

The Fig. 1 show the orographies for the domains used in the dynamical downscaling process. The left figure represents the domain for the 1st step of dynamical downscaling. Using the data from this simulation, the model was run for the domain shown on the right hand side in the Fig. 1.

20   ## 3   Simulations and results

The ECHAM5-HAM model was run for the time period of 1 July 2004–31 December 2005. The data output frequency used was 6 h and instantaneous values of the tracers were written out. From these results, the lateral tracer boundary data for REMO-HAM were processed, as described in Sect. 2.5.1. The REMO model was run for time pe-

25   riod of 1 October 2004–31 December 2005 for the 0.44° (50 km) resolution with a time

step of 240 s, and 1 December 2004–31 December 2005 for the 0.088° (10 km) resolution using 50 s time step. The model was run with the normal version (REMO) and with the aerosol module version (REMO-HAM). The time periods were chosen so that ECHAM5-HAM has 3 months of spin up time for the tracers, REMO/REMO-HAM with 50 km resolution has 2 months of spin up time and REMO/REMO-HAM with 10 km resolution has 1 month. In this work, we have only used the binary sulfuric acid – water based nucleation method by Kazil and Lovejoy (2007) for both of the models.

ECHAM5-HAM and REMO-HAM included a slightly improved dry deposition scheme. The dry deposition scheme calculates dry deposition velocities separately for vegetated surface, wet skin, bare soil or snow, water and ice (Ganzeveld and Lelieveld, 1995; Ganzeveld et al., 1998). It has been updated to use separate values of virtual potential temperature, roughness length and stability functions over land, water and ice rather than gridbox averages of these quantities in the calculation of dry deposition velocities. (Actually the virtual potential temperature was erroneously taken from the value for land, which is assigned a default value over water or ice.) This results in a significant strengthening of the dry deposition sink for some species, for example in ECHAM5-HAM, global dry deposition of SO_2 increased from 17.6 Tg(S) yr^{-1} before the changes to 20.8 Tg(S) yr^{-1} afterwards (cf. a total emission flux of 71 Tg(S) yr^{-1}). We have used this updated scheme on all of the simulations done in this work.

We have compared our results to measurement data from CREATE (Construction, use and delivery of an European aerosol database)[1] and EBAS [2] databases. From this dataset, we have chosen 4 different measurement sites: Hyytiälä (Finland 62° N and 24′ E), Melpitz (Germany 51° N and 13′ E), Mace Head (Ireland 53° N and 10′ W) and Jungfraujoch (Switzerland 47° N and 8′ E). From these stations, only the Melpitz and Jungfraujoch sites are within the 10 km resolution domain.

From Hyytiälä (Dal Maso et al., 2005) and Melpitz (Birmili and Wiedensohler, 2000) stations we have used the Differential Mobility Particle Sizer (DMPS) data for the to-

---

[1]http://www.nilu.no/projects/ccc/create/

[2]http://ebas.nilu.no

tal number concentrations and size distributions. For Jungfrajoch Collaud Coen et al. (2007, 2011) and Mace Head (O'Connor et al., 2008), Condensation Particle Counter (CPC) data was used for total number concentration. In addition, from Mace Head the aerosol size distributions were measured with Scanning Mobility Particle Sizer (SMPS).

⁵ The gas phase SO_2 concentrations are also compared against measurements. For Mace Head, there are no measurements of SO_2. As a proxy for Mace Head, we have used data from Valentia Observatory which is located approximately 150 km due South-West from the Mace Head measurement station (Bashir et al., 2006). The data from Valentia is daily filter data and should represent the concentrations from Mace Head
¹⁰ quite reasonably. The time resolution of one day was also used in the gas phase measurements from Jungfraujoch. For Hyytiälä and Melpitz, the gas phase data has a 30 min time resolution.

From all the four measurement sites, Jungfraujoch is the the only one located in a mountainous area (the Alps) as can be seen from the Fig. 2. In the case of Hyytiälä,
¹⁵ Melpitz and Mace Head, the results from the models are from the lowest model layer. The mountainous location of Jungfraujoch makes the analysis a bit different: the altitude of the station is 3580 m and the closest model level matching this has been used (the model level was actually calculated based on the pressure levels). This has been done, because the models use the σ-hybrid coordinates for the vertical levels, which
²⁰ means that levels follow the terrain in the lower troposphere (but become pure pressure coordinates in the higher altitudes). The model orography for the Alpine region is flatter than the reality, especially in the case of ECHAM5-HAM. This means that the lowest model layer does not describe the actual measurement station altitude and thus the closest matching pressure level has been chosen. The level has been calculated
²⁵ separately for each of the models due to the different orography.

3.1 Aerosol total number concentrations

Figure 3 presents the measured and modelled weekly aerosol total number concentrations for different measurement sites. We can see that for Hyytiälä ECHAM5-HAM re-

produces the aerosol concentrations quite reasonably. The modelled values are slightly lower than measured, especially during late winter, early summer and autumn, but the yearly cycle is fairly well captured. REMO-HAM has a similar yearly cycle to the measurements, but the fluctuations in concentrations are higher. In some cases, the concentration peaks are higher than the measurement or results from ECHAM5-HAM, but overall REMO-HAM gives lower concentrations. In any case, the values from the models are fairly close to the measurements. On the other hand, in the current setup for the models we did not include any boundary layer (BL) nucleation scheme (although implemented). BL nucleation could be one of the factors that could improve the models performance during spring and autumn, which are typical nucleation event times at Hyytiälä (Dal Maso et al., 2005). The reason why we did not include BL nucleation is explained in the Sect. 3.1.2. Moreover, Spracklen et al. (2006) showed that either BL nucleation or primary emissions can not directly explain the measured concentration at Hyytiälä, but the sum of these is the best fit to the measurements. This means that the models would give higher concentrations during spring, summer and autumn. It could also probable that there would be some overestimation in number concentrations. From Fig. 4 we can see that the number concentrations between different modes, except for the nucleation and Aitken mode, does not differ much at Hyytiälä. Aitken mode is smaller with REMO-HAM during the whole year, which can explain the differences in the Fig. 3. The nucleation mode concentrations are a bit higher in REMO-HAM, but the difference is not very big. The differences in Aitken mode concentrations are discussed in Sect. 3.1.2.

The results from Melpitz show that the models give lower concentration than the measurements throughout the whole year and that the difference between the models is quite small. The difference between the two different REMO-HAM resolutions is barely discernible. Unlike at Hyytiälä, the nucleation mode concentrations differ the most. On the other hand, the Aitken mode concentrations are much higher and it dominates the total number concentrations (Fig. 4). This is why the difference in nucleation mode is not visible in the total number concentrations. The missing BL nucleation may

The regional aerosol-climate model REMO-HAM

J.-P. Pietikäinen et al.

Back | Close

Full Screen / Esc

Printer-friendly Version

Interactive Discussion

be an important factor when we consider why the models give too low total number concentrations at Melpitz.

At Mace Head, ECHAM5-HAM reproduces the measured values fairly well during the first half of the year, but underestimates the concentrations during the second half. REMO-HAM has the same pattern, although during late winter and spring time the concentrations are lower than in ECHAM5-HAM and measurements. Fig. 4 shows that the difference between ECHAM5-HAM and REMO-HAM comes from the nucleation mode, which is lower in REMO-HAM during the first quarter of the year, and in summer and autumn.

As mentioned in Sect. 3, the Jungfraujoch measurement site is located in a mountainous region (The Alps). These kind of areas are demanding for the model and the results have greater error than usual, which can be seen from Fig. 3. The concentrations given by the models are too high throughout the year. ECHAM5-HAM has somewhat higher concentrations than REMO-HAM. The 10 km resolution simulation has slightly higher concentrations, but the difference between the resolutions is not very significant. The difference between ECHAM5-HAM and REMO-HAM (50 km) in nucleation mode can be seen from Fig. 4 and the interesting point is that the nucleation mode concentrations are very high compared to other measurement sites. The reason for this is explained later on.

Figures 3 and 4 show the number concentrations only from the lowest model layer, except for Jungfraujoch where the model level has been matched to the measurement by pressure. In this work, we have not included vertical measurement data, but we have compared ECHAM5-HAM and REMO-HAM (50 km resolution). From Fig. 5 we see how the vertical distribution of particle number changes seasonally. ECHAM5-HAM has higher concentrations at all sites below 750 hPa. Above this, REMO-HAM has higher concentrations at Hyytiää and Melpitz, excluding the highest pressure levels (close to the surface). Also noticeable is that total number concentrations get higher until around 300 hPa and then starts to decrease. This kind of behavior has been previously observed in ECHAM5-HAM by Kazil et al. (2010). The reason for this is the

The regional aerosol-climate model REMO-HAM

J.-P. Pietikäinen et al.

Back | Close

Full Screen / Esc

Printer-friendly Version

Interactive Discussion

high concentration in the nucleation mode, which can be seen from Fig. 6 (note: these values are annual means which smooths out differences when compared to seasonal values). We can see how the nucleation mode dominates the total number concentrations from 200 hPa to 900 hPa. REMO-HAM has somewhat higher concentrations in all of the modes (with some fluctuations), except the nucleation mode, which is higher in ECHAM5-HAM. At higher altitudes, the difference is not noticeable anymore. Also interesting is the effect of coarser orography at Jungfraujoch with ECHAM5-HAM. We can see that the values of REMO-HAM does not reach as high pressure levels as with ECHAM5-HAM. The low horizontal resolution tends to smoothen the orographical differences and that is why REMO-HAM has better representation of the Alps (lowest values are in higher altitudes than with ECHAM5-HAM). Figure 6 also shows why the nucleation mode concentration is so high at Jungfraujoch in Fig. 3. As mentioned, Jungfraujoch station is located at the Alps and the values in Fig. 3 were chosen based on the pressure levels (higher altitude). This leads to higher nucleation mode concentrations at Jungfraujoch station. Why the nucleation mode concentrations are increasing at higher altitudes can be an effect of various different reasons, as described by Kazil et al. (2010). For example, the too high SO_2 concentrations can lead to too high H_2SO_4 concentrations, which affects the nucleation, the oxidation processes may influence on the H_2SO_4 budget and the treatment of ultrafine particles in M7 in terms of the mode limits can have an effect on the concentrations.

3.1.1 Aerosol size distributions

As mentioned in the previous section, the nucleation mode can explain the difference in total number concentrations between the models at almost all of the measurement sites. The high concentrations in the nucleation mode can be also seen in Fig. 7, where the yearly mean size distributions from Hyytiälä, Melpitz and Mace Head as well as the modeled mean distributions are shown. Results from Hyytiälä show that the distributions from the models are quite similar to the measurements, except for small particles, which are overestimated. The width of the distribution is not quite captured, although

ECHAM5-HAM has wider distribution than with REMO-HAM. The peak is almost in the right place for both of the models and ECHAM5-HAM has the height of the main peak very well captured, whereas REMO-HAM underestimates the concentrations. At Mace Head, similar behavior can be seen, although both of the models underestimate the concentration of the larger particles. The noticeable difference is that ECHAM5-HAM has more particles in the smallest sizes, which is in accord with the spring and summer time higher nucleation mode concentrations as seen in Fig. 4. At Melpitz, we can see features similar to the other sites, but the form of the distributions gives some clue why the models differ. It seems that in the case of ECHAM5-HAM, the gas phase sulfuric acid has condensed more on the particles and this has lead to smaller nucleation mode and to the higher and wider distribution. In the next section we will explain this in more detail.

3.1.2 Nucleation mode and gas phase

In this work, the boundary layer nucleation was not used. However, the neutral and charged H_2SO_4/H_2O nucleation by Kazil and Lovejoy (2007) was used in both of the models during the simulation period. In this approach, the nucleation rate depends on the sulfuric acid concentration. The source for gas phase sulfate is the oxidation processes of SO_2 and DMS, as described in Sect. 2.3. The concentrations of SO_2 (especially in continental areas) are much higher than those of DMS, and thus it is the main proxy for gas phase sulfate production (Hamed et al., 2010). The difference in the nucleation mode between ECHAM5-HAM and REMO-HAM could be explained by higher nucleation rates, which would be the results of higher sulfate (sulfuric acid) concentrations due to the different SO_2 concentrations.

Figure 8 shows the SO_2 gas phase concentrations for all the measurement sites and models (here the results from Valentia, Ireland, instead of Mace Head are shown). It is quite clear that both of the models overestimate the SO_2 concentrations at all of the measurement sites. At Hyytiälä, REMO-HAM has higher values than measurements, especially during winter and early spring. ECHAM5-HAM has similar values

754

for the beginning of the year, although in some rare cases being slightly lower than in REMO-HAM. Later on, values with REMO-HAM decrease, but are still higher than the measurements. ECHAM5-HAM also has a decreasing slope, but the values start to increase during the summer and are too high especially during the late autumn and winter. At Melpitz, the values are quite high in both of the models. The total number concentrations were underestimated at Melpitz and the reason for this is the low concentration in the nucleation mode. Although at Melpitz SO_2 concentrations are high, the nucleation mode number concentration is not, because there is not enough sulfuric acid to activate nucleation. The reason for this is the Aitken mode. As we can see from Fig. 4, the Aitken mode is quite high at Melpitz. This leads to a larger condensation sink, which in turn leads to low sulfuric acid concentrations. This can be also seen from Fig. 7, where the nucleation peaks are low at Melpitz, but the otherwise the distribution is high and wide. In case of REMO-HAM, the condensation sink is lower and there is more sulfuric acid to activate nucleation. This can be seen from Figs. 4 and 7. The reason for differences in Aitken mode are most probably due to emissions, which differ because of the differing model resolutions.

As previously mentioned, the model versions used included some changes to dry deposition, which decreased the SO_2 concentrations. If we look closer how the nucleated particles grow in M7, the only condensing substance (besides water) is sulfuric acid. It seems that when the SO_2 concentrations decrease closer to the measured values, the sulfuric acid concentration decrease as well and the condensation is not anymore high enough to grow the particles. This can be seen from the Fig. 7, where the nucleation mode has high peaks on every measurement site.

The boundary layer nucleation was not used in this work, because the sulfuric acid concentrations were so high. BL nucleation schemes are very sensitive to H_2SO_4 concentration and without condensation of organic matter (SOA model), the nucleation mode concentrations would be unrealistic high. We are currently working with problem of too high SO_2 and H_2SO_4 concentrations in another projects.

Figure 9 shows the zonal and yearly means for Europe for sulfate production rates and sulfuric acid concentrations for both of the models. We see that the production rates are fairly similar in liquid and gas phase. The biggest difference is that in ECHAM5-HAM, the production rates are higher at higher altitudes. This is connected to the SO_2 concentrations, which are also higher in ECHAM5-HAM. The sulfuric acid (H_2SO_4) concentrations are somewhat lower in REMO-HAM, but the pattern similar to ECHAM5-HAM. In any case, based on Fig. 9, we can say that the main processes in REMO-HAM for H_2SO_4 are working as they should. Small differences, like seen in the nucleation mode concentration in Fig. 4, can be explained by normal fluctuations arising from the different model resolutions.

3.1.3 Spatial variability

We can see from Fig. 10 how the different resolution of the models changes the spatial distribution of the total number concentration. The values shown are the mean values over summer months (June, July and August) and for the lowest models layer. The difference in details between ECHAM5-HAM and REMO-HAM (50 km) is considerable, although the main features of spatial distribution can be seen from both. The values are fairly similar for different areas, which was also shown in Fig. 3. If the two different REMO-HAM resolutions are compared, the difference is quite small. Some of the very local concentration peaks are different, but the main feature of the spatial distribution is more or less identical. This is because of two main reasons: firstly, the higher resolution was driven by the lower resolution simulation and secondly, the emissions database was same for both of the simulations and it had coarser resolution than either of the model versions. It is quite clear that if we want to use the full benefit of the high resolution, the emission database needs to be updated, at least in terms of the spatial resolution. It should be also mentioned that higher resolution in time has the potential to bring further differences between different model resolutions (now most of the species use monthly fields). In any case, the Fig. 10 shows how much the higher

Full Screen / Esc

Printer-friendly Version

Interactive Discussion

resolution of regional aerosol-climate model can improve the spatial presentation of the aerosol concentrations.

3.2 Meteorological variables

We have compared the meteorological model results with the Climatic Research Unit (CRU, http://www.cru.uea.ac.uk/) data. The data used is the CRU TS 3.0 global dataset with 0.5° resolution. The dataset only has measurement data over land so all sea areas are excluded. We have compared the dataset with the precipitation and temperature from ECHAM5-HAM, REMO and REMO-HAM. The model data has been remapped to the CRU grid. We have used conservative remapping for precipitation fields and bilinear remapping for temperature. The temperature fields are also adjusted according to different orographies between CRU and the models. We have used the lapse rate $\gamma = 0.0064 \,°C \, m^{-1}$ to fix the orography difference in temperatures. The remapping has been done for the ECHAM5-HAM global T63 grid and REMO 0.44° grid.

Figure 11 shows the temperature difference (model-measurements) for each of the models. We can see that ECHAM5-HAM is quite close to the measurements throughout Europe. This is of course an expected result since we were using the nudging method for the ECHAM5-HAM simulation. On the other hand, the REMO and REMO-HAM simulations were not nudged (they were only driven by the ECMWF analysis data at the lateral boundaries), and as we can see, both of the models seems to reproduce the measured values fairly well. REMO has a small cold bias over Eastern Europe whereas in REMO-HAM this is hardly perceptible. Both of the models have warm bias over Western Europe, especially with REMO-HAM, which seems to overestimate the temperatures much more than REMO. Some of the areas with high bias are located in polluted areas and a radiation scheme including HAM-M7 aerosol information would be a valuable addition to the model. Direct effect of aerosols can play an important role, especially on a regional scale.

Figure 12 shows the precipitation difference ((model-measurements)/measurements) for each of the models. ECHAM5-HAM seems to have wet bias over Eastern

and Central Europe, and dry bias over some parts of Western Europe, North Africa and Middle East. REMO and REMO-HAM have the same pattern, but the biases are not as high as with ECHAM5-HAM. REMO is overall more closer to the measurements than REMO-HAM, which has too wet bias, especially over Eastern Europe. The pattern of precipitation between the models is quite similar. REMO and REMO-HAM have systematic precipitation difference along the boundaries, which is an effect of the relaxation scheme (prognostic variables are adjusted within eight outermost grid boxes). The large-scale driving field influence deacreases expotentially from the outermost boundary towards the center of the domain.

REMO-HAM currently uses the same autoconversion parameters as used in ECHAM5-HAM with a resolution scaling factor. These scaling factors change the autoconversion parameters according to the resolution and have an impact on the precipiation. The effect of the scaling parameters should be studied further, and this is ongoing work.

4   Conclusions

We have performed simulations with regional aerosol-climate regional model REMO-HAM with two different resolutions: $50 \times 50 \, \text{km}^2$ and $10 \times 10 \, \text{km}^2$. In addition, we have done simulations with the global aerosol-climate model ECHAM5-HAM. The simulation were done for the year 2005 taking into account spin-up time. The aerosol related tracer data from ECHAM5-HAM simulation were used as lateral boundary data for REMO-HAM. ECHAM5-HAM was nudged with ECMWF operational analysis data and REMO-HAM used the same data at the lateral boundaries of the model domain.

The results from both of the models were compared against aerosol measurements from four different measurement sites. We have shown that the REMO-HAM can represent the measured aerosol concentrations and size distributions fairly realistically. Overall the concentrations are somewhat low, but one has to keep in mind that this version of REMO-HAM does not include an online SOA-model, and that boundary layer

nucleation was not used. With ECHAM5-HAM, the total number concentrations shows the same patterns as REMO-HAM. The difference between the models can be mainly explained by the nucleation mode, which differs in time and space. The nucleation mode is linked to the sulfur dioxide concentrations through oxidation and nucleation. We have shown that the models tend to overestimate the sulfur dioxide concentrations and this leads to high nucleation rates. In some cases, like at Melpitz, the background concentration of aerosol was high enough to increase the condensation of sulfuric acid to particles and this lead to lower nucleation rates. We have implemented some improvements to the models in terms of dry deposition. These improvements led to lower sulfur dioxide and sulfuric acid levels, but raised a new problem: the condensation of sulfuric acid is not anymore high enough to grow the smaller particles to larger sizes. One thing missing from REMO-HAM is the growth of particles by organic matter. ECHAM5-HAM has a secondary organic aerosol version (O'Donnell et al., 2011), but it was not used in this study. Since the aerosol module structure is similar in both of the models, we will study the option of implementing the SOA model to REMO-HAM.

Emissions are the dominant factor for number concentrations in the lowest model layers. In this study, we tested REMO-HAM with two different horizontal resolutions (0.44° and 0.088°). Differences in the aerosol concentrations are small between the two REMO-HAM simulations, as both use the same emission fields. This means that although REMO-HAM with 0.088° resolution is able to solve the circulation with much higher accuracy, the coarse emissions were a restricting factor for the aerosol concentrations. In order to use high resolution aerosol-climate models for detailed studies, a high resolution emissions dataset should be used.

Temperature and precipitation fields from REMO-HAM was evaluated by comparing the parameters to CRU observation. REMO-HAM captures the annual mean temperature reasonably well, but overestimates the precipitation amount in most regions. The meteorology of the model will be studied more thoroughly in forthcoming publications (for example, the effect of scaling parameter to the autoconversion parameters). Moreover, the difference in sulfur species will be studied in more detail in the future.

References

Abdul-Razzak, H. and Razzak, S. J.: A parameterization of aerosol activation 2. Multiple aerosol types, J. Geophys. Res., 105, D5, 6837–6844, 2000. 746

Bashir, W., Ryan, M., Burke, L., McGovern F., and Paull B.: An analysis of the ionic composition of Irish precipitation and background air quality since 1980 based on samples collected at Valentia Observatory, Co. Kerry, Ireland, Air Pollution XIV, 545–555, 2006. 750

Beheng K. D.: A parametrization of warm cloud microphysical conversion processes, Atmos. Res., 33, 193–206, 1994. 746

Birmili, W. and A. Wiedensohler.: New particle formation in the continental boundary layer: meteorological and gas phase parameter influence, Geophys. Res. Lett., 27, 3325–3328, 2000. 749

Collaud Coen, M., Weingartner, E., Nyeki, S., Cozic, J., Henning, S., Verheggen, B., Gehrig, R. and Baltensperger, U.: Long-term trend analysis of aerosol variables at the high-alpin site Jungfraujoch, J. Geophys. Res., 112, D13213, doi:10.1029/2006JD007995, 2007. 750

Collaud Coen, M., Weingartner, E., Furger, M., Nyeki, S., Prévôt, A. S. H., Steinbacher, M., and Baltensperger, U.: Aerosol climatology and planetary boundary influence at the Jungfraujoch analyzed by synoptic weather types, Atmos. Chem. Phys., 11, 5931–5944, doi:10.5194/acp-11-5931-2011, 2011. 750

Croft, B., Lohmann, U., Martin, R. V., Stier, P., Wurzler, S., Feichter, J., Posselt, R., and Ferrachat, S.: Aerosol size-dependent below-cloud scavenging by rain and snow in the ECHAM5-HAM, Atmos. Chem. Phys., 9, 4653–4675, doi:10.5194/acp-9-4653-2009, 2009. 747

Dal Maso, M., Kulmala, M., Riipinen, I., Wagner, R., Hussein, T., Aalto, P. P., and Lehtinen, K. E. J.: Formation and growth of fresh atmospheric aerosols: eight years of aerosol

The regional aerosol-climate model REMO-HAM

J.-P. Pietikäinen et al.

size distribution data from SMEAR II, Hyytiala, Finland, Boreal Environ. Res., 10(5), 323–336, 2005. 749, 751

Davies, H. C.: A lateral boundary formulation for multi-level prediction models, Q. J. Roy. Meteor. Soc., 102, 405–418, 1976. 747

5   Dentener, F., Kinne, S., Bond, T., Boucher, O., Cofala, J., Generoso, S., Ginoux, P., Gong, S., Hoelzemann, J. J., Ito, A., Marelli, L., Penner, J. E., Putaud, J.-P., Textor, C., Schulz, M., van der Werf, G. R., and Wilson, J.: Emissions of primary aerosol and precursor gases in the years 2000 and 1750 prescribed data-sets for AeroCom, Atmos. Chem. Phys., 6, 4321–4344, doi:10.5194/acp-6-4321-2006, 2006. 740, 744, 745

10   Feichter, J., Kjellström, E., Rodhe, H., Dentener, F., Lelieveld, J., and Roelofs, G.-J.: Simulation of the tropospheric sulfur cycle in a global climate model, Atmos. Environ., 30, 1693–1707, 1996. 744

Ganzeveld, L. and J. Lelieveld.: Dry deposition parameterization in a chemistry general circulation model and its influence on the distribution of reactive trace gases, J. Geophys. Res., 15   100, D10, 20999–21012, 1995. 749

Ganzeveld, L., Lelieveld, J., and Roelofs, G.-J.: A dry deposition parameterization for sulfur oxides in a chemistry and general circulation model, J. Geophys. Res., 103, D5, 5679–5694, 1998. 749

Hamed, A., Birmili, W., Joutsensaari, J., Mikkonen, S., Asmi, A., Wehner, B., Spindler, G., Jaati- 20   nen, A., Wiedensohler, A., Korhonen, H., Lehtinen, K. E. J., and Laaksonen, A.: Changes in the production rate of secondary aerosol particles in Central Europe in view of decreasing SO_2 emissions between 1996 and 2006, Atmos. Chem. Phys., 10, 1071–1091, doi:10.5194/acp-10-1071-2010, 2010. 754

Hansen, J., Sato, M., and Ruedy, R.: Radiative forcing and climate response, J. Geophys. Res., 25   102, 6831–6864, 1997. 739

Haywood, J. M. and Boucher, O.: Estimates of the direct and indirect radiative forcing due to tropospheric aerosols: a review, Rev. Geophys., 38, 513–543, 2000. 739

Horowitz, L. W., Walters, S., Mauzerall, D. L., Emmons, L. K., Rasch, P. J., Granier, C., Tie, X., Lamarque, J.-F., Schultz, M. G., Tyndall, G. S., Orlando, J. J., and Brasseur, G. P.: A global 30   simulation of tropospheric ozone and related tracers: description and evaluation of MOZART, version 22, J. Geophys. Res., 108, 4784, doi:10.1029/2002JD002 853, 2003. 744

IPCC, Intergovernmental Panel on Climate Change: Climate Change 2007: Synthesis Report, Cambridge Univ. Press, 2007. 740

Title Page

Abstract | Introduction

Conclusions | References

Tables | Figures

◄ | ►►

◄ | ►

Back | Close

Full Screen / Esc

Printer-friendly Version

Interactive Discussion

Jacob, D.: A note to the simulation of the annual and inter-annual variability of the water budget over the Baltic Sea drainage basin, Meteorol. Amtos. Phys., 77, 61–73, 2001. 742

Jacob, D. and Podzun, R.: Sensitivity studies with the Regional Climate Model REMO, Meteorol. Amtos. Phys., 63, 119–129, 1996. 741, 742

5 Jacobson, M. Z., Tabazadeh, A., and Turco R. P.: Simulating equilibrium within aerosols and nonequilibrium between gases and aerosols, J. Geophys. Res., 101(D4), 9079–9091, 1996. 743

Jones, A., Roberts, D. L., and Slingo, A.: A climate model study of indirect radiative forcing by anthropogenic sulphate aerosols, Nature, 370, 450–453, 1994. 741

10 Kazil, J. and Lovejoy, E. R.: A semi-analytical method for calculating rates of new sulfate aerosol formation from the gas phase, Atmos. Chem. Phys., 7, 3447–3459, doi:10.5194/acp-7-3447-2007, 2007. 743, 749, 754

Kazil, J., Stier, P., Zhang, K., Quaas, J., Kinne, S., O'Donnell, D., Rast, S., Esch, M., Ferrachat, S., Lohmann, U., and Feichter, J.: Aerosol nucleation and its role for clouds and

15 Earth's radiative forcing in the aerosol-climate model ECHAM5-HAM, Atmos. Chem. Phys., 10, 10733–10752, doi:10.5194/acp-10-10733-2010, 2010. 752, 753

Khairoutdinov, M. and Kogan, Y.: A new cloud physics parameterization in a large-eddy simulation model of marine stratocumulus, Mon. Weather Rev., 128, 229–243, 2000. 746

Kokkola, H., Korhonen, H., Lehtinen, K. E. J., Makkonen, R., Asmi, A., Järvenoja, S., Anttila, T.,

20 Partanen, A.-I., Kulmala, M., Järvinen, H., Laaksonen, A., and Kerminen, V.-M.: SALSA – a Sectional Aerosol module for Large Scale Applications, Atmos. Chem. Phys., 8, 2469–2483, doi:10.5194/acp-8-2469-2008, 2008. 741

Kokkola, H., Hommel, R., Kazil, J., Niemeier, U., Partanen, A.-I., Feichter, J., and Timmreck, C.: Aerosol microphysics modules in the framework of the ECHAM5 climate model – intercom-

25 parison under stratospheric conditions, Geosci. Model Dev., 2, 97–112, doi:10.5194/gmd-2-97-2009, 2009. 744

Kulmala, M., Vehkamäki, H., Petäjä, T., Dal Maso, M., Lauri, A., Kerminen, V.-M., Birmili, W., and McMurry, P. H.: Formation and growth rates of ultrafine atmospheric particles: a review of observations, J. Aerosol. Sci., 35, 143–176, 2004. 740

30 Kulmala, M., Lehtinen, K. E. J., and Laaksonen, A.: Cluster activation theory as an explanation of the linear dependence between formation rate of 3nm particles and sulphuric acid concentration, Atmos. Chem. Phys., 6, 787–793, doi:10.5194/acp-6-787-2006, 2006. 743

Title Page

Abstract | Introduction

Conclusions | References

Tables | Figures

◄ | ►

◄ | ►

Back | Close

Full Screen / Esc

Printer-friendly Version

Interactive Discussion

Laakso, L., Anttila, T., Lehtinen, K. E. J., Aalto, P. P., Kulmala, M., Hõrrak, U., Paatero, J., Hanke, M., and Arnold, F.: Kinetic nucleation and ions in boreal forest particle formation events, Atmos. Chem. Phys., 4, 2353–2366, doi:10.5194/acp-4-2353-2004, 2004. 743

Laaksonen, A., Hamed, A., Joutsensaari, J., Hiltunen, L., Cavalli, F., Junkermann, W., Asmi, A., Fuzzi, S., and Facchini, M. C.: Cloud condensation nucleus production from nucleation events at a highly polluted region, Geophys. Res. Lett., 32, L06812, doi:10.1029/2004GL022092, 2005. 740

Langmann, B.: Numerical modelling of regional scale transport and photochemistry directly together with meteorological processes, Atmos. Environ., 34, 3585–3598, 2000. 747

Langmann, B., Varghese, S., Marmer, E., Vignati, E., Wilson, J., Stier, P., and O'Dowd, C.: Aerosol distribution over Europe: a model evaluation study with detailed aerosol micro-physics, Atmos. Chem. Phys., 8, 1591–1607, doi:10.5194/acp-8-1591-2008, 2008. 741

Lin, H. and Leaitch, W. R.: Development of an in-cloud aerosol activation parameterization for climate modelling. In: Proceedings of the WMO Workshop pn Measurement of Cloud Properties for Forecast of Weather, Air Quality and Climate, World Meteorol. Organ., Geneva, 328–335, 1997. 746

Lohmann, U. and Feichter, J.: Global indirect aerosol effects: a review, Atmos. Chem. Phys., 5, 715–737, doi:10.5194/acp-5-715-2005, 2005. 740

Lohmann, U. and Kärcher, B.: First interactive simulations of cirrus clouds formed by homoge-neous freezing in the ECHAM general circulation model, J. Geophys. Res., 107, D10, 4105, doi:10.1029/2001JD000767, 2002. 746

Lohmann, U. and Roeckner, E.: Design and performance of a new cloud microphysics scheme developed for the ECHAM genereal circulation model, Clim. Dynam., 12, 557–572, 1996. 746

Lohmann, U., Stier, P., Hoose, C., Ferrachat, S., Kloster, S., Roeckner, E., and Zhang, J.: Cloud microphysics and aerosol indirect effects in the global climate model ECHAM5-HAM, Atmos. Chem. Phys., 7, 3425–3446, doi:10.5194/acp-7-3425-2007, 2007. 741, 746

Lohmann, U., Spichtinger, P., Jess, S., Peter, T., and Smit, H.: Cirrus cloud formation and ice supersaturated regions in a global climate model, Environ. Res. Lett., 3, 045022, doi:10.1088/1748–9326/3/4/045022, 2008. 746

Louis, J.-F.: A parametric model of vertical eddy fluxes in the atmosphere, Bound.-Lay. Meteorol. 17, 187–202, 1979. 747

Title Page

Abstract | Introduction

Conclusions | References

Tables | Figures

◀ | ▶

◀ | ▶

Back | Close

Full Screen / Esc

Printer-friendly Version

Interactive Discussion

Makkonen, R., Asmi, A., Korhonen, H., Kokkola, H., Järvenoja, S., Räisänen, P., Lehtinen, K. E. J., Laaksonen, A., Kerminen, V.-M., Järvinen, H., Lohmann, U., Bennartz, R., Feichter, J., and Kulmala, M.: Sensitivity of aerosol concentrations and cloud properties to nucleation and secondary organic distribution in ECHAM5-HAM global circulation model, Atmos. Chem. Phys., 9, 1747–1766, doi:10.5194/acp-9-1747-2009, 2009. 741

Mellor, B. and Yamada, T.: A hierarchy of turbulence closure models for planetary boundary layers, J. Atmos. Sci., 31, 1791–1806, 1974. 747

Nordeng, T. E.: Extended versions of the convective parametrization scheme at ECMWF and their impact on the mean and transient activity of the model in Tropics, ECMWF Tech. Memo., 206, Available from ECMWF, Shineld Park, Reading, RG2 9AX, UK, 1994. 742

O'Connor, T. C., Jennings, S. G., and O'Dowd, C. D.: Highlights of fifty years of atmospheric aerosol research at Mace Head, Atmos. Res., 90(2–4), 338–355, 2008. 750

O'Donnell, D., Tsigaridis, K., and Feichter, J.: Estimating the direct and indirect effects of secondary organic aerosols using ECHAM5-HAM, Atmos. Chem. Phys., 11, 8635–8659, doi:10.5194/acp-11-8635-2011, 2011. 741, 743, 759

Petters, M. D. and Kreidenweis, S. M.: A single parameter representation of hygroscopic growth and cloud condensation nucleus activity, Atmos. Chem. Phys., 7, 1961–1971, doi:10.5194/acp-7-1961-2007, 2007. 743

Pfeifer, S.: Modeling cold cloud processes with the regional climate model REMO, PhD. Thesis, Reports on Earth System Science, Max Planc Institute for Meteorology, Hamburg, 2006. 742

Pleim, J. E., Chang, J. S., and Zhang, K. S.: A nested grid mesoscale atmospheric chemistry model, J. Geophys. Res., 96, 3065–3084, 1991. 747

Raatikainen, T., Vaattovaara, P., Tiitta, P., Miettinen, P., Rautiainen, J., Ehn, M., Kulmala, M., Laaksonen, A., and Worsnop, D. R.: Physicochemical properties and origin of organic groups detected in boreal forest using an aerosol mass spectrometer, Atmos. Chem. Phys., 10, 2063–2077, doi:10.5194/acp-10-2063-2010, 2010. 740

Roeckner, E., Arpe, K., Bengtsson, L., Christoph, M., Claussen, M., Dumenil, L., Esch, M., Schlese, U., and Schulzweida, U.: The atmospheric general circulation model ECHAM4: Model description and simulation of present-day climate, Max Planck Institute for Meteorology report series, Report No. 218, Hamburg, Germany, 1996. 742

Roeckner, E., Baeuml, G., Bonventura, L., Brokopf, R., Esch, M., Giorgetta, M., Hagemann, S., Kirchner, I., Kornblueh, L., Manzini, E., Rhodin, A., Schlese, U., Schulzweida, U., and Tompkins, A.: The atmospheric general circulation model ECHAM5. PART I: Model description,

The regional aerosol-climate model REMO-HAM

J.-P. Pietikäinen et al.

Max Planck Institute for Meteorology report series, Report No. 349, Hamburg, Germany, 2003. 741

Seinfeld, J. and Pandis, S.: Atmospheric Chemistry and Physics, John Wiley & Sons inc., New York, USA, 1998. 740

5 Smolarkiewicz, P. K.: Simple positive definite advection scheme with small implicit diffusion, Mon. Weather Rev., 111, 479–486.1, 1983. 747

Smolarkiewicz, P. K.: A fully multidimensional positive definite advection transport algorithm with small implicit diffusion, J. Comput. Phys., 54, 325–362.1, 1984. 747

Sogacheva, L., Dal Maso, M., Kerminen., V.-M., and Kulmala, M.: Probability of nucleation
10 events and estimation of aerosol particle sources at Hyytiälä, Southern Finland, using back trajectories, Boreal Environ. Res., 10 479–491, 2005. 740

Sogacheva, L., Hamed, A., Facchini, M. C., Kulmala, M., and Laaksonen, A.: Relation of air mass history to nucleation events in Po Valley, Italy, using back trajectories analysis, Atmos. Chem. Phys., 7, 839–853, doi:10.5194/acp-7-839-2007, 2007. 740

15 Spracklen, D. V., Carslaw, K. S., Kulmala, M., Kerminen, V.-M., Mann, G. W., and Sihto, S.-L.: The contribution of boundary layer nucleation events to total particle concentrations on regional and global scales, Atmos. Chem. Phys., 6, 5631–5648, doi:10.5194/acp-6-5631-2006, 2006. 741, 751

Stier, P., Feichter, J., Kinne, S., Kloster, S., Vignati, E., Wilson, J., Ganzeveld, L., Tegen, I.,
20 Werner, M., Balkanski, Y., Schulz, M., Boucher, O., Minikin, A., and Petzold, A.: The aerosol-climate model ECHAM5-HAM, Atmos. Chem. Phys., 5, 1125–1156, doi:10.5194/acp-5-1125-2005, 2005. 741, 743, 744, 747, 767

Sundqvist, H.: A parameterization scheme for non-convective condensation including prediction of cloud water content, Q. J. Roy. Meteor. Soc., 104, 677–690, 1978.

25 Sundqvist, H., Berge, E., and Kristiansson, J. E.: Condensation and cloud parameterization studies with a mesoscale numerical weather prediction model, Mon. Weather Rev., 117, 1641–1657, 1989. 742, 746

Tanre, D., Geleyn, J.-F., and Slingo, J. M.: First results of the introduction of an advanced aerosol-radiation interaction in the ECMWF low resolution global model, in: Aerosols and
30 their Climatic Effects, edited by: Gerber, H. and Deepak, A., 133–177, A. Deepak, Hampton, Virginia, 1984. 742

Tiedtke, M.: A comprehensive mass flux scheme for cumulus parametrisation in large-scale models, Mon. Weather Rev., 117, 1779–1800, 1989. 742

The regional aerosol-climate model REMO-HAM

J.-P. Pietikäinen et al.

Vehkamäki, H., Kulmala, M., Napari, I., Lehtinen, K. E. J., Timmreck, C., Noppel, M., and Laaksonen, A.: An improved parameterization for sulfuric acid-water nucleation rates for tropospheric and stratospheric conditions, J. Geophys. Res., 107, 4622, doi:10.1029/2002JD002184, 2002. 743

5 Vignati, E., Wilson, J., and Stier, P.: M7: An efficient size-resolved aerosol microphysics module for large-scale aerosol transport models, J. Geophys. Res., 109, D22202, doi:10.1029/2003JD004485, 2004. 741, 743

Zubler, E. M., Folini, D., Lohmann, U., Lüthi, D., Muhlbauer, A., Pousse-Nottelmann, S., Schär, C., and Wild, M.: Implementation and evaluation of aerosol and cloud microphysics

10 in a regional climate model, J. Geophys. Res., 116, D02211, doi:10.1029/2010JD014572, 2011. 741

The regional aerosol-climate model REMO-HAM

J.-P. Pietikäinen et al.

Title Page

Abstract	Introduction
Conclusions	References
Tables	Figures

|◄ | ►|

◄ | ►

Back | Close

Full Screen / Esc

Printer-friendly Version

Interactive Discussion

Table 1. The modal structure of HAM-M7. N_i denotes the aerosol number of mode i and M_i^j denotes the mass of compound j. The dry radius r shows the limits of different modes (Stier et al., 2005).

Mode	Soluble/Mixed	Insoluble
Nucleation mode $r \leq 5\,\mathrm{nm}$	N_1, M_1^S	
Aitken mode $5\,\mathrm{nm} < r \leq 50\,\mathrm{nm}$	$N_2, M_2^S, M_2^{BC}, M_2^{POM}$	N_5, M_5^{BC}, M_5^{POM}
Accumulation mode $50\,\mathrm{nm} < r \leq 0.5\,\mu\mathrm{m}$	$N_3, M_3^S, M_3^{BC}, M_3^{POM}, M_3^{SS}, M_3^{DU}$	N_6, M_6^{DU}
Coarse mode $0.5\,\mu\mathrm{m} < r$	$N_4, M_4^S, M_4^{BC}, M_4^{POM}, M_4^{SS}, M_4^{DU}$	N_7, M_7^{DU}
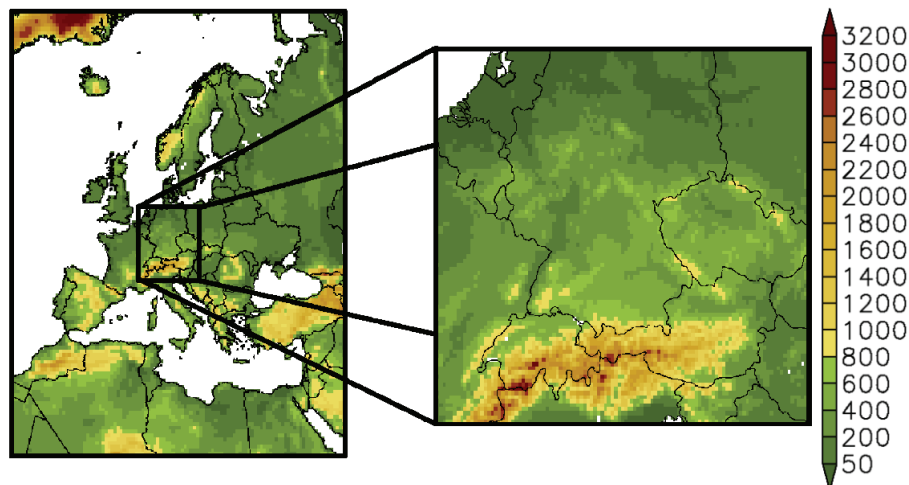
Fig. 1. The orogpraphies of the used domains in meters. On the left hand side the 0.44° resolution domain and on the right hand side the 0.088° resolution domain.
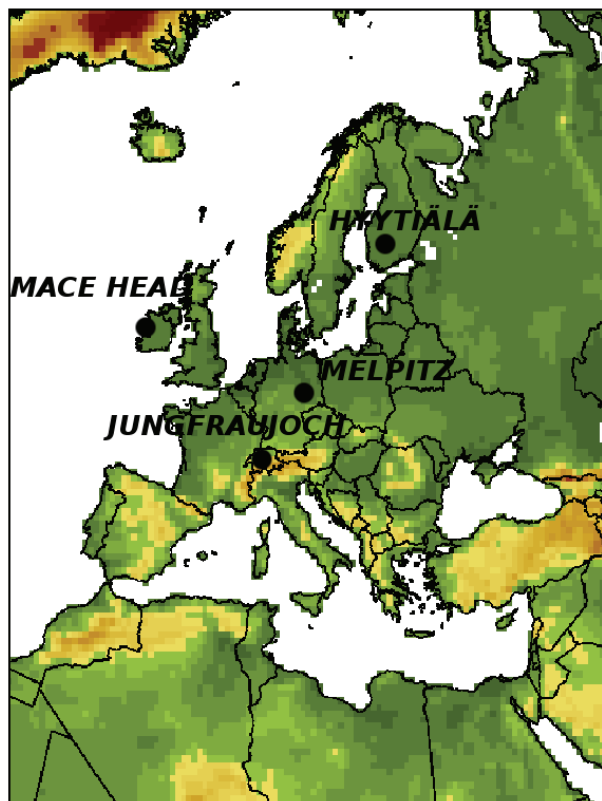
Fig. 2. The selected CREATE database stations: Hyytiälä, Melpitz, Mace Head and Jungfrau-joch.

Full Screen / Esc

Printer-friendly Version

Interactive Discussion
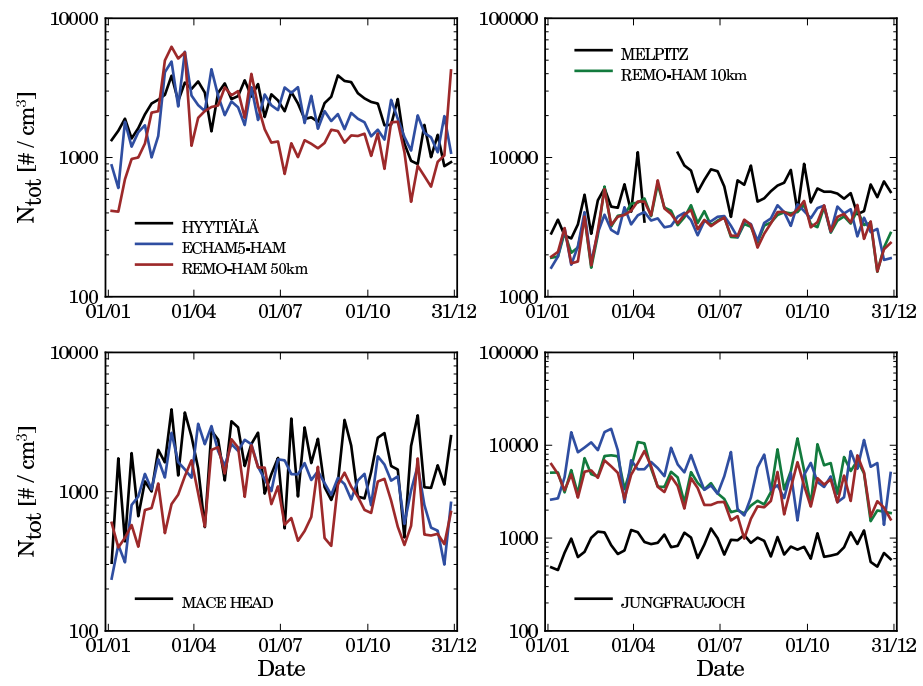
Fig. 3. The weekly mean total number concentrations from different measurements sites and models as a function of time.
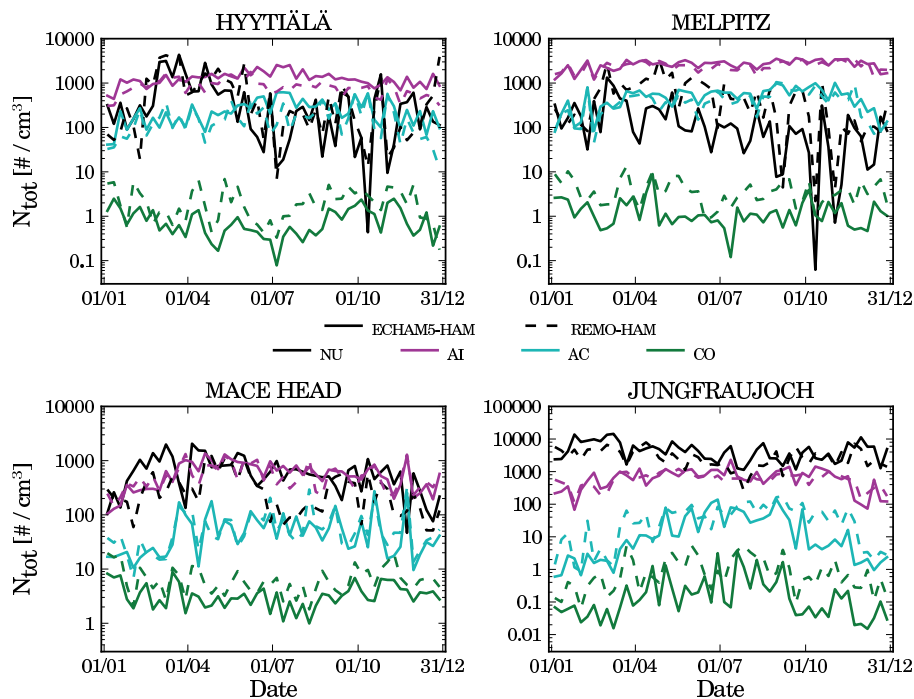
Fig. 4. The weekly mean number concentrations for nucleation (NU), Aitken (AI), accumulation (AC) and coarse (CO) mode. The values from ECHAM5-HAM are represented by the solid lines (–) and REMO-HAM (50 km resolution) by the dashed lines (– –).
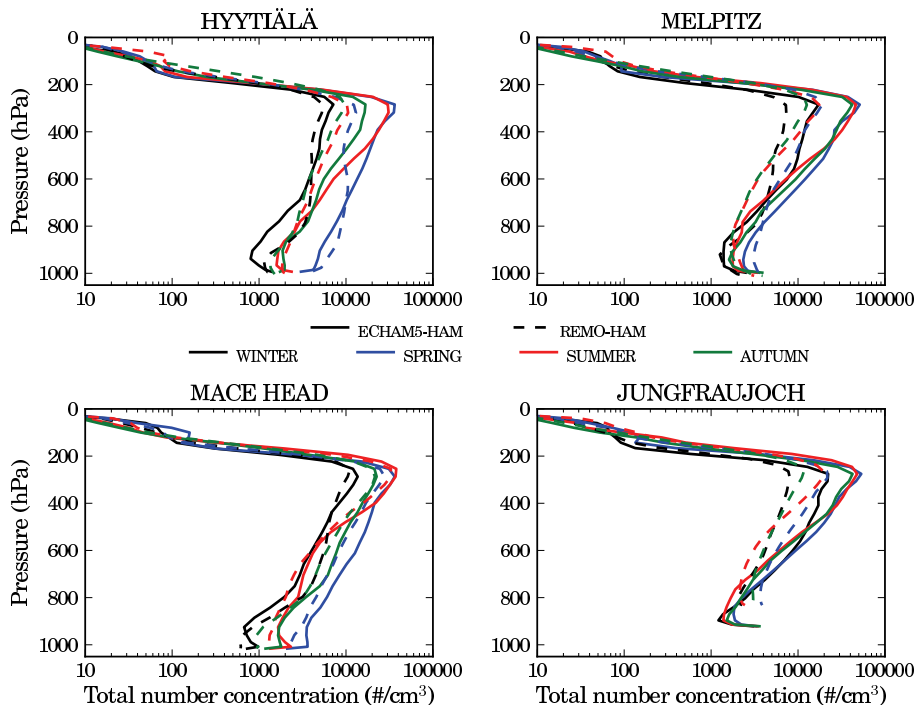
Fig. 5. The seasonal mean number concentrations as a function of pressure. The values from ECHAM5-HAM are represented by the solid lines (–) and REMO-HAM (50 km resolution) by the dashed lines (– –).
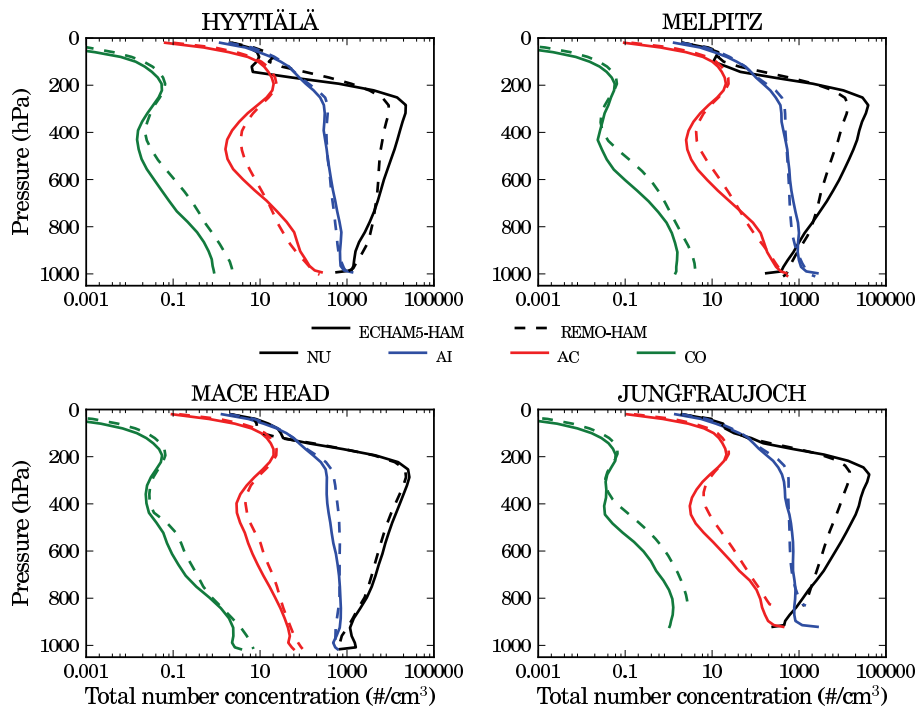
Fig. 6. The yearly mean number concentrations for different modes as a function of pressure: nucleation (NU), Aitken (AI), accumulation (AC) and coarse (CO) mode. The values from ECHAM5-HAM are represented by the solid lines (–) and REMO-HAM (50 km resolution) by the dashed lines (– –).
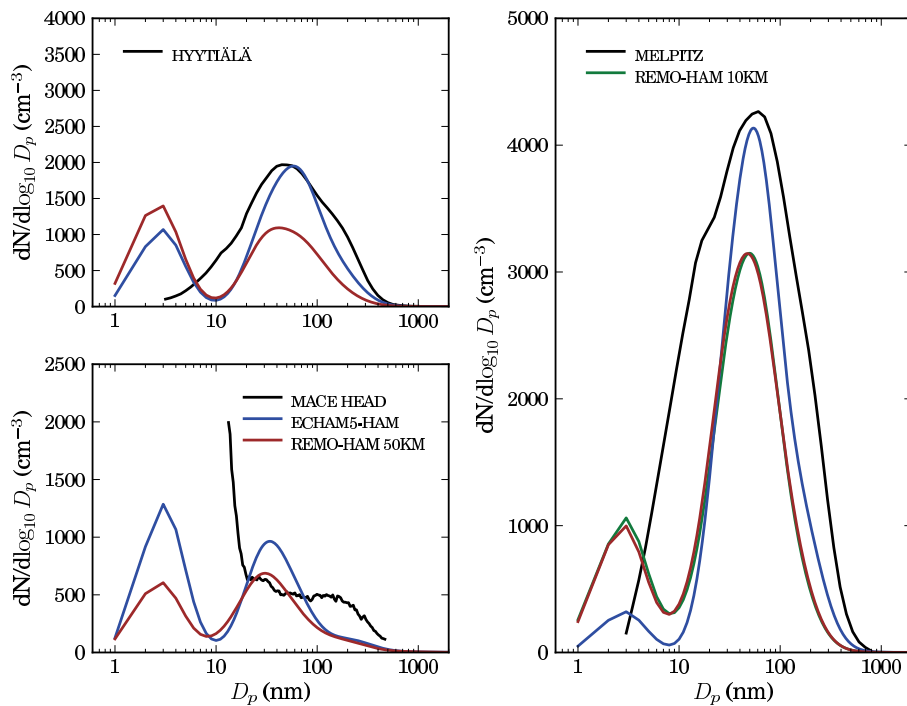
Fig. 7. The yearly mean aerosols size distributions from three measurements sites.

The regional aerosol-climate model REMO-HAM

J.-P. Pietikäinen et al.

Title Page

Abstract	Introduction
Conclusions	References
Tables	Figures

Back | Close

Full Screen / Esc

Printer-friendly Version

Interactive Discussion
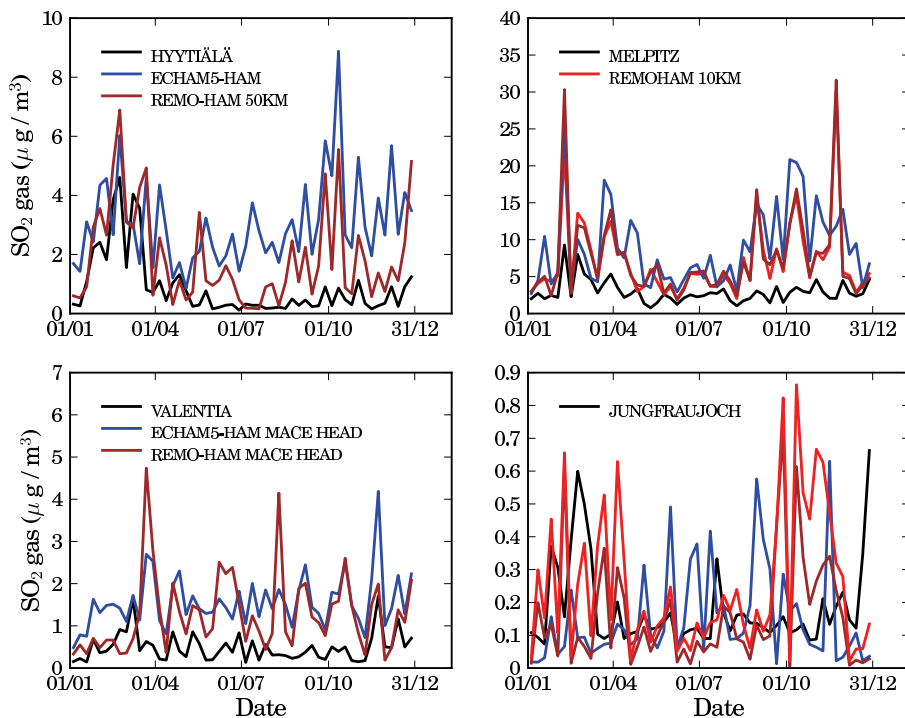
Fig. 8. The weekly mean SO_2 gas phase concentration from different measurement sites as a function of time. For Mace Head, the measured values from Valentia are shown.
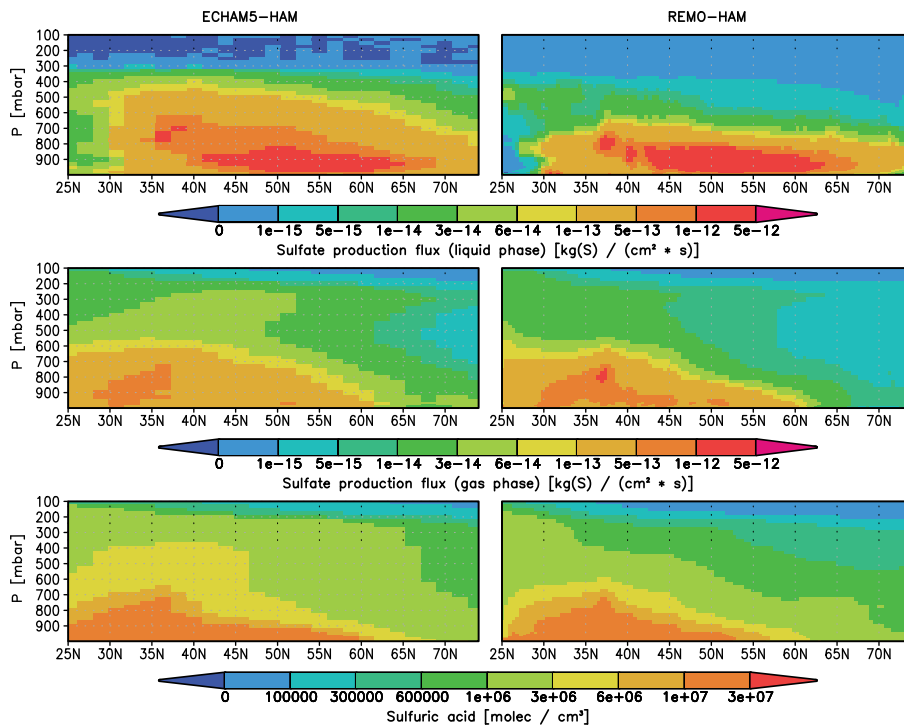
Fig. 9. Zonal mean sulfate production fluxes (upper panel for liquid phase and central for gas phase) and zonal mean sulfuric acid concentrations (lower panel) for the year 2005: ECHAM5-HAM on the left column and REMO-HAM on the right column.

Title Page

Abstract   Introduction

Conclusions   References

Tables   Figures

◄   ►

◄   ►

Back   Close

Full Screen / Esc

Printer-friendly Version

Interactive Discussion
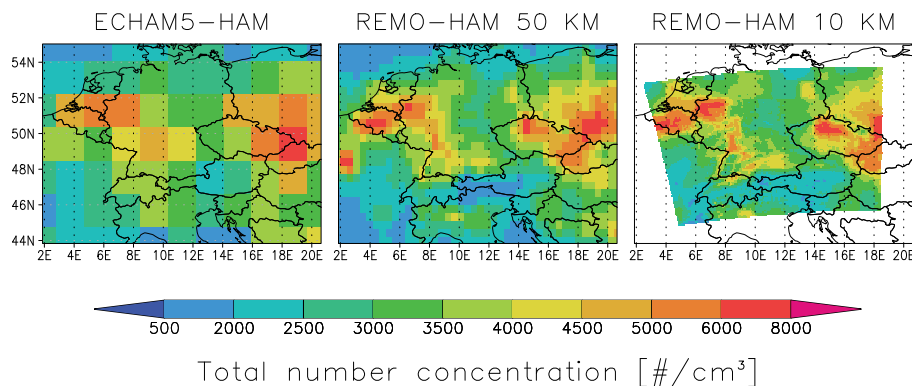
Fig. 10. The mean aerosol total number concentration for the different models. Only the values from the lowest model layer are shown and the values are mean over the summer months (June, July and August).
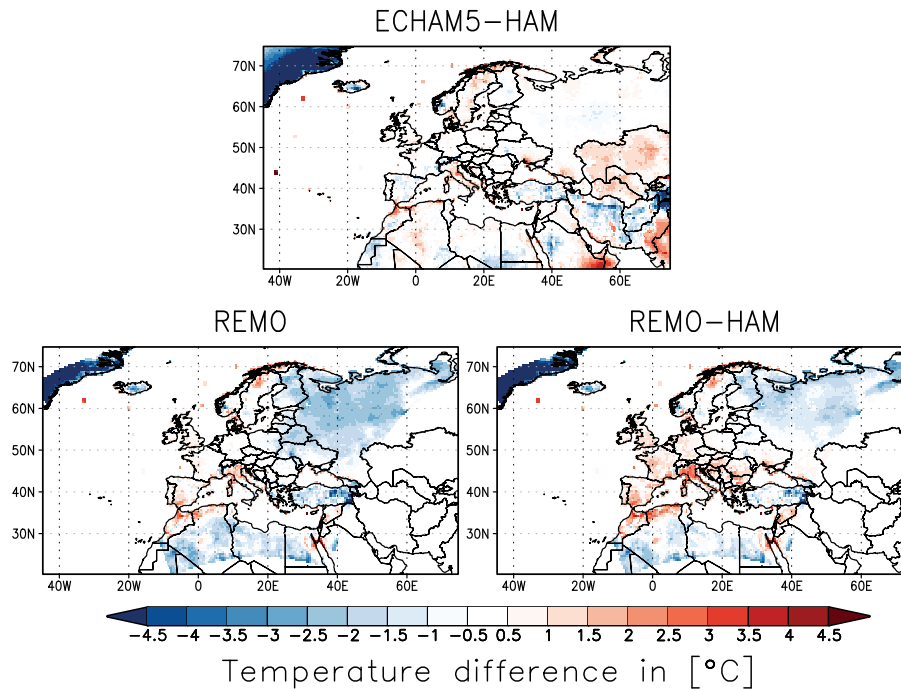
Fig. 11. Temperature difference (model-measurements) for ECHAM5-HAM, REMO and REMO-HAM.
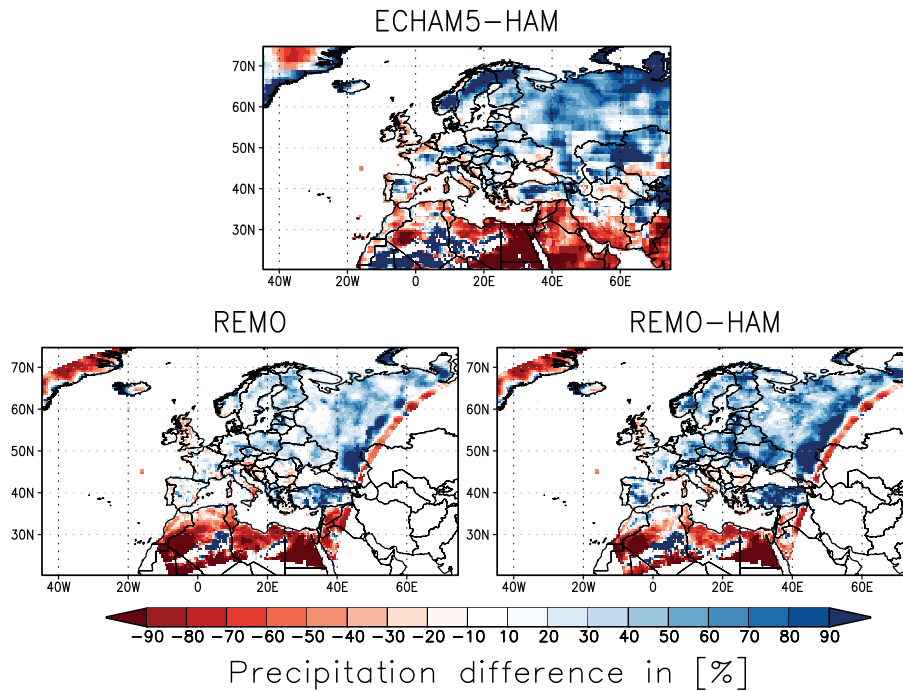
Fig. 12. Precipitation difference ((model-measurements)/measurements ×100 %) for ECHAM5-HAM, REMO and REMO-HAM.